International Journal of Pharmaceutics 618 (2022) 121638

Contents lists available at ScienceDirect

International Journal of Pharmaceutics

journal homepage: www.elsevier.com/locate/ijpharm

Utilizing *in vitro* drug release assays to predict *in vivo* drug retention in micelles

Aida Varela-Moreira [a,b], Heleen van Leur [b], Danielle Krijgsman [b], Veronika Ecker [c], Martina Braun [c], Maike Buchner [c], Marcel H.A.M. Fens [b,*], Wim E. Hennink [b], Raymond M. Schiffelers [a,b]

[a] CDL Research, University Medical Center Utrecht, Utrecht, the Netherlands
[b] Department of Pharmaceutics, Utrecht Institute for Pharmaceutical Sciences (UIPS), Faculty of Science, Utrecht University, Utrecht, the Netherlands
[c] Institute for Clinical Chemistry and Pathobiochemistry, School of Medicine, Technical University Munich, Munich, Germany

ARTICLE INFO

Keywords:
Polymeric micelles
Drug delivery
Hydrophobic drugs
In vitro - in vivo correlation
Circulation kinetics
3R principle

ABSTRACT

In the present work, we aim at developing an *in vitro* release assay to predict circulation times of hydrophobic drugs loaded into polymeric micelles (PM), upon intravenous (i.v.) administration. PM based on poly (ethylene glycol)-b-poly (N-2-benzoyloxypropyl methacrylamide) (mPEG-b-p(HPMA-Bz)) block copolymer were loaded with a panel of hydrophobic anti-cancer drugs and characterized for size, loading efficiency and release profile in different release media. Circulation times in mice of two selected drugs loaded in PM were evaluated and compared to the *in vitro* release profile. Release of drugs from PM was evaluated over 7 days in PBS containing Triton X-100 and in PBS containing albumin at physiological concentration (40 g/L). The results were utilized to identify crucial molecular features of the studied hydrophobic drugs leading to better micellar retention. For the best and the worst retained drugs in the *in vitro* assays (ABT-737 and BCI, respectively), the circulation of free and entrapped drugs into PM was examined after i.v. administration in mice. We found *in vivo* drug retention at 24 h post-injection similar to the retention found in the *in vitro* assays. This demonstrates that *in vitro* release assay in buffers supplemented with albumin, and to a lesser degree Triton X-100, can be employed to predict the *in vivo* circulation kinetics of drugs loaded in PM. Utilizing media containing acceptor molecules for hydrophobic compounds, provide a first screen to understand the stability of drug-loaded PM in the circulation and, therefore, can contribute to the reduction of animals used for circulation kinetics studies.

1. Introduction

Many drugs and drug candidates have poor aqueous solubility (Kalepu and Nekkanti, 2015; Lipinski, 2000; Takagi et al., 2006). This is a challenge for drug development, as these drugs are difficult to formulate. To improve aqueous solubility, and to avoid the need of toxic organic solvents, the formulation of poorly water-soluble drugs in nanoparticles is a frequently explored method (Kalepu and Nekkanti, 2015). One class of nanoparticles able to solubilize hydrophobic drugs is polymeric micelles (PM), which are prepared from amphiphilic block copolymers that self-assemble in a core–shell structure and allow accommodation of poorly water-soluble drugs in this core (Jones and Leroux, 1999; Varela-Moreira et al., 2017; Deng et al., 2012; Cabral et al., 2018). Besides the increase of drug solubility in aqueous milieu, micellar encapsulation can also improve circulation time of drugs in blood after systemic administration. Prolonged circulation is facilitated by the hydrophilic shell, generally composed of poly (ethylene glycol) (PEG), sterically stabilizing PM's surface in biological media. Furthermore, this hydrophilic shell also delays PM recognition by cells of the mononuclear phagocyte system. The prolonged circulation of PM paves the road for target site accumulation by exploiting the enhanced permeability and retention (EPR) effect (Lammers, 2019; Maeda et al., 2000). Improved target site accumulation, and/or reduced accumulation in healthy tissues, improves the therapeutic window of the loaded drug.

The clinical translation of PM remains challenging as only a few formulations have granted approval for use in patients (Varela-Moreira et al., 2017; Houdaihed et al., 2017a). The main challenges are the

* Corresponding author at: Department of Pharmaceutics, Utrecht Institute for Pharmaceutical Sciences (UIPS), Utrecht University, Universiteitslaan 99, 3584 CG, Utrecht, The Netherlands.
E-mail address: m.h.a.m.fens@uu.nl (M.H.A.M. Fens).

https://doi.org/10.1016/j.ijpharm.2022.121638
Received 23 December 2021; Received in revised form 28 February 2022; Accepted 2 March 2022
Available online 5 March 2022

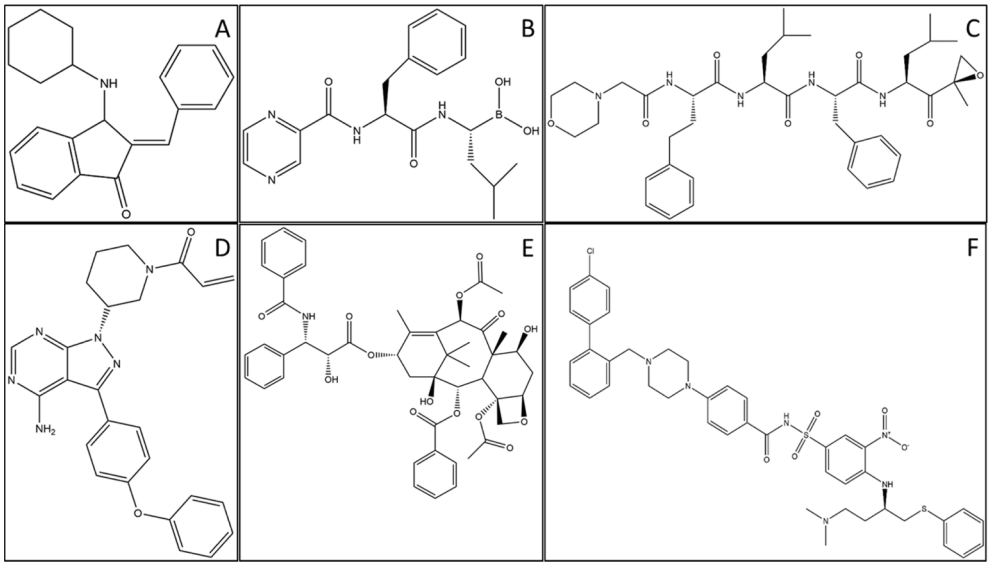

Fig. 1. Chemical structures of the drugs used in this study and loaded in polymeric micelles. (A) BCI, (B) bortezomib, (C) carfilzomib, (D) ibrutinib, (E) paclitaxel and (F) ABT-737.

Table 1
Physicochemical properties of hydrophobic drugs loaded in polymeric micelles.

Name of the drug	Molecular Weight* (g/mol)	Number of Aromatic Groups*	LogP*	Number of Rotatable Bonds*	Charge* at pH 7.4
BCI	317	2	4.94	3	0.89
bortezomib	384	2	1.53	9	−0.05
carfilzomib	720	2	4.20	20	0.00
paclitaxel	854	3	3.54	14	0.00
ibrutinib	441	4	3.63	5	0.00
ABT-737	813	5	7.48	15	0.88

*molecular properties retrieved from Chemicalize (Anonymous) (ChemAxon, Budapest, Hungary).

limited *in vivo* stability and drug retention after intravenous (i.v.) administration, both essential for EPR effect-mediated drug delivery (Kim et al., 2010; Wilhelm et al., 2016). The stability of PM upon venous administration can be compromised due to the dilution of PM below the critical micelle concentration (CMC) leading to their dissociation and/or due to the interaction of the hydrophobic segment of the block copolymer with plasma proteins such as albumin, also known as the biomolecular corona (Sharifi et al., 2020; Cai and Chen, 2019). PM stability can be improved by various methods, based on non-covalent (Yuan et al., 2001; Shi et al., 2017) and covalent interactions (van Nostrum, 2011). Most employed covalent stabilization methods are based on crosslinking of either the core or the shell of PM. This can efficiently stabilize the micellar structure in biological environment and increase the circulation time of the micelles. However, chemical crosslinking strategies are frequently not compatible with the loaded drug (Talelli et al., 2012). Chemical conjugation can be challenging as careful optimization for each drug-polymer combination is needed and therapeutic efficacy can likely be compromised due to insufficient drug release from PM (Talelli et al., 2012; Talelli et al., 2010; Yokoyama et al., 1998). Regarding non-covalent stabilization methods, increasing stability through hydrophobic interactions and through π-π stacking, appear very attractive because of their relatively high strength (Zhuang et al., 2019). For π-π stacking-based interactions, the presence of aromatic moieties in the backbone of the drug and in the hydrophobic domains of the polymer are essential. This strategy is also attractive as no modification of drug or polymer are required. We have previously shown that PM based on methoxy poly (ethylene glycol)-block-(N-(2-benzoyloxypropyl) methacrylamide) (mPEG-b-p(HPMA-Bz)) attain good loading and retention of paclitaxel (PTX, three aromatic groups) and docetaxel (DTX, two aromatic groups) (Shi et al., 2015). It was suggested that the major stabilizing force is π-π stacking between the aromatic moieties present in the drug and in the p(HPMA-Bz) block.

In the present study, we investigated the release profiles of several poorly-water soluble anti-cancer drugs loaded into PM in Triton X-100 and albumin-containing media and compared these to the circulation time in mice upon i.v. administration. Additionally, the impact of different molecular properties of drugs on the loading and retention in mPEG-b-p(HPMA-Bz)-based PM was analyzed. Six hydrophobic drugs with varying molecular weight, logP and number of aromatic moieties were selected and loaded in PM (Fig. 1 and Table 1). These four drugs and two drug candidates loaded into PM comprised bortezomib (Velcade®), carfilzomib (Kyprolis®), paclitaxel (Taxol®) and ibrutinib (Imbruvica®), (E)-2-Benzylidene-3-(cyclohexylamino)-2,3-dihydro-1H-inden-1-one (BCI) and ABT-737, respectively. To simplify we will indicate both the selected drugs and drug candidates as 'drugs' throughout this study. Drug-loaded PM were characterized for size, loading efficiency, and loading content. The *in vitro* release profile of tested drugs was determined in two different release media containing Triton X-100 and albumin as agents (acceptor molecules) that 'capture' the released drugs in the medium, thereby facilitating so called sink conditions. Finally, the circulation time after systemic administration of best and worst retained drugs, ABT-737 and BCI, loaded into PM was assessed and compared to their release profiles found in the *in vitro* assays. With this comparison we aim to investigate whether the *in vitro* release assay can predict *in vivo* circulation of hydrophobic drugs. If so, one can reduce the number of animals for laboratory experimentation. Poor drug retention in PM lead to low drug concentrations at the target site which, in turn, will compromise the therapeutic effect. Thus, the retention of drugs in PM upon systemic administration is a key evaluation step to identify promising formulations for further investigation (Sakai-Kato et al., 2015; Houdaihed et al., 2017a; Houdaihed et al., 2017b; Lee et al., 2010).

Here we aim to test the translatability of an *in vitro* release assay in biological media to predict drug retention in PM *in vivo*. With this assay, we can contribute to decrease the number of animals needed for circulation kinetic studies. Overall, we aim to reduce (one of the 3R's) the number of animals used for circulation kinetic studies.

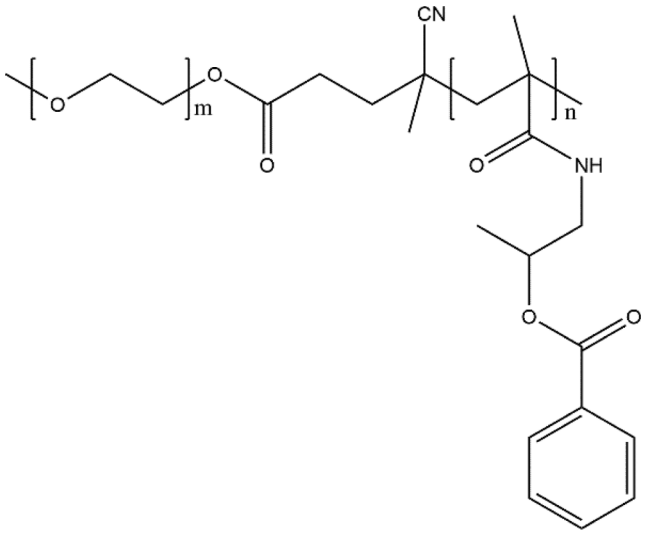

Fig. 2. Chemical structure of mPEG-b-p(HPMA-Bz) used for preparation of the drug loaded polymeric micelles. M_n of the block copolymer was 22 kDa, mPEG was 5 kDa. The block copolymer was synthesized with HPMA-Bz as monomer and mPEG2-ABCPA as initiator Bagheri et al., 2018.

2. Animals, materials and methods

2.1. Animals

A total of 15 C57BL/6NRj mice (Janvier Labs, France), gender indifferent, 6–12-week-old with an average body weight of 21 ± 1 g were used in this study. Mice were housed in IVC blue line cages (Tecniplast Spa, Buguggiate, Italy) with 5 mice per cage in a light–dark cycle of 12 h/12 h at a temperature of 21 ± 2 °C. Food and water were provided *ad libitum*. Cage enrichment was provided with shredded autoclaved paper, mouse house and wood bricks (Tecniplast Spa, Buguggiate, Italy).

All animal work was conducted in accordance with German Federal Animal Protection Laws and approved by the Institutional Animal Care and Use Committee at the Technical University of Munich and is reported according to the ARRIVE Guidelines.

2.2. Materials

All organic solvents were from Biosolve Ltd. (Valkenswaard, the Netherlands), and the chemicals used in this study were purchased from Sigma-Aldrich (Zwijndrecht, the Netherlands) unless mentioned otherwise. Water was purified to Milli-Q water by Synergy UV water purification system (Merck Millipore, Darmstadt, Germany). Dialysis cassettes Float-A-Lyzer G2 purchased from Repligen Corporation (Boston, MA, USA). Filters of 0.45 µm regenerated cellulose membrane were purchased from Phenomenex, Utrecht, the Netherlands. Bovine serum albumin (BSA) purchased from Sigma Aldrich, Zwijndrecht, the Netherlands. HPLC and UPLC columns and equipment were supplied by Waters Associates Inc., Milford, MA, USA. Bortezomib, carfilzomib, ibrutinib and paclitaxel were obtained from LC Laboratories (Woburn, MA, USA), BCI from Axon Medchem (Groningen, the Netherlands) and ABT-737 from AdooQ BioScience (Irvine, CA, USA).

2.3. Methods

2.3.1. Preparation and characterization of polymeric micelles

PM were prepared using mPEG-b-p(HPMA-Bz) copolymer (M_n of 22 kDa, mPEG of 5 kDa) prepared with HPMA-Bz as monomer and $mPEG_2$-ABCPA as macroinitiator (Fig. 2) (Bagheri et al., 2018). In brief, 30 mg of the synthesized block copolymer and drug (amounts varied from 0.5 to 20 mg) were dissolved in 1 mL of tetrahydrofuran (THF) (Shi et al., 2015). Then, the polymer/drug solution was added dropwise to 1 mL of water under agitation for 1 min at room temperature. The micellar dispersion was subsequently incubated overnight in a fume hood to allow evaporation of THF. Next, the volume was adjusted to 1 mL with 10x concentrated HEPES-buffered saline (HBS) (200 mM HEPES, 1500 mM sodium chloride, pH 7.4) to yield micellar dispersions in HBS at final concentration of 20 mM HEPES, 150 mM sodium chloride, pH 7.4. The PM dispersions were filtered through an 0.45 µm filter membrane to remove any precipitated/non encapsulated drug. The size of PM was determined by dynamic light scattering (DLS) after 10x dilution in water at 25 °C (ZetaSizer Nano ZS 90, Malvern Analytical, UK). Mean Z-averaged particle size and polydispersity index (PDI) were obtained using supplier's software.

To determine the amount of the loaded drug, one volume of PM was added to nine volumes of acetonitrile (ACN) to disrupt the PM and solubilize the drug content. ABT-737 micelles were destabilized in at least a 10-fold volume ACN/MeOH (1:1). The samples were subsequently analyzed by HPLC (Waters Alliance System), with a SunFire C18 column (5 µm, 4.6 × 150 mm) or UPLC (Waters ACQUITY System) using an ACQUITY BEH C18 column (1.7 µm, 2.1 × 50 mm). HPLC and UPLC methods for detection and quantitation of the different drugs are reported in the Supporting Information. Loading efficiency and loading content were calculated as follows:

$$Loading\ efficiency\ \% = Weight\ loaded\ drug / Weight\ feed\ drug \times 100\%$$

$$Loading\ content\ \% = Weight\ loaded\ drug / Weight\ (loaded\ drug + polymer) \times 100\%$$

Loading capacity value for each drug is defined as the highest loading content, meaning the maximum weight of drugs that can be loaded in PM.

2.3.2. Drug release from polymeric micelles

The drug release assays were performed in Float-A-Lyzer G2 dialysis cassettes of 100 kDa molecular weight cut-off (MWCO) using 2% v/v Triton X-100 in phosphate buffered saline (PBS, containing 11.9 mM phosphate, 137 mM sodium chloride and 2.5 mM potassium chloride) as the releasing medium (Naksuriya et al., 2015). In brief, 30 mL of 2% v/v Triton X-100 in PBS was added to 50 mL tubes and the dialysis cassette subsequently loaded with 1 mL of drug-loaded PM was put inside the tube. These were well sealed and let rotating at 4 or 37 °C. At predefined time points – 1, 2, 4, 6, 8, 24, 48, 72, 96, 120, 144 and 168 h - aliquots of 10 µL were collected from inside the dialysis cassette and analyzed by HPLC or UPLC as described in supporting information (SI).

Drug release in bovine serum albumin (40 g/L in PBS) was conducted similarly, unless stated here. The molar albumin/drug ratio was calculated based on the amount of drug loaded in PM used in this assay. The molar ratio of albumin/drug was between 2 and 30 mol/mol. Since one albumin molecule binds to two drug molecules (Sudlow et al., 1975, 1976), the albumin-to-drug ratios used in this study are sufficient to solubilize the released drug molecules. The dialysis cassette used had a MWCO of 300 kDa to allow albumin molecules to freely distribute/diffuse between the inside of the dialysis cassette and the external releasing medium. To maintain osmotic equilibrium, 0.5 mL of drug-loaded PM and 0.5 mL of albumin solution were added to the dialysis cassette. To separate the drug from albumin, 90 µL of ACN was added to the 10 µL aliquots, vortexed for 1 min and subsequently the precipitated albumin was spun down at 12,000*g* for 10 min. The supernatant was collected and analyzed by HPLC/UPLC according to analytical methods for each drug described in SI. This method was validated by spiking known amounts of drug with albumin, followed by precipitation of albumin and determination of the drug concentration in the supernatant.

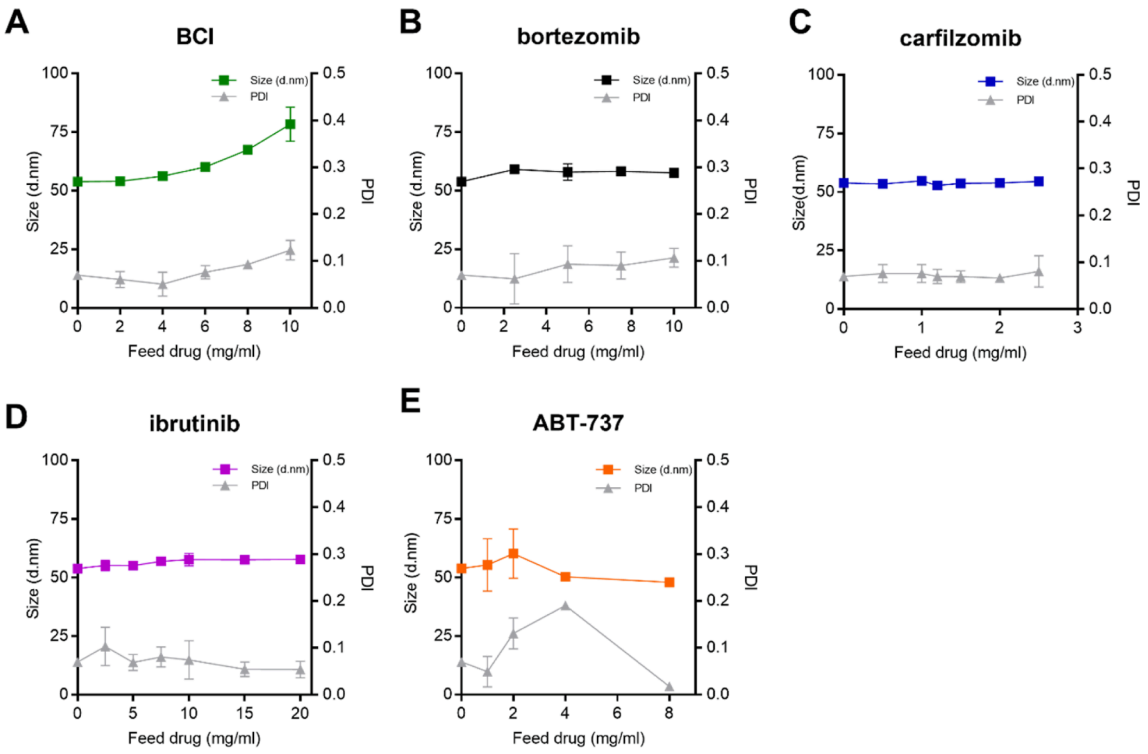

Fig. 3. Size and Polydispersity Index of polymeric micelles loaded with hydrophobic drugs. The size is the Z-average diameter as determined by DLS after 10× dilution of the micellar dispersion in water. PDI is the polydispersity index of the polymeric micelles. Data are shown as mean ± SD, n = 3.

Full recover of the added drugs was achieved.

2.3.3. *Circulation time of drug loaded in Cy7-labeled micelles*

Circulation time of ABT-737 and BCI loaded Cy7-labelled PM were assessed using immunocompetent C57BL/6NRj mice. Mice were i.v. injected with 100–200 μL of ABT-737-PM (1 mg/mL of drug; 30 mg/mL of polymer) and BCI-PM (6 mg/mL of BCI; 30 mg/mL of polymer) via the tail vein. Blood was withdrawn via submandibular puncture at 1 min (considered as 100% of the injected dose), 1 and 24 h after injection and collected in lithium-heparin coated tubes. At any single occasion no more than 5% of the total blood volume was withdrawn. On 25-gram mice, this corresponds to 70 μL of blood. Plasma was obtained by

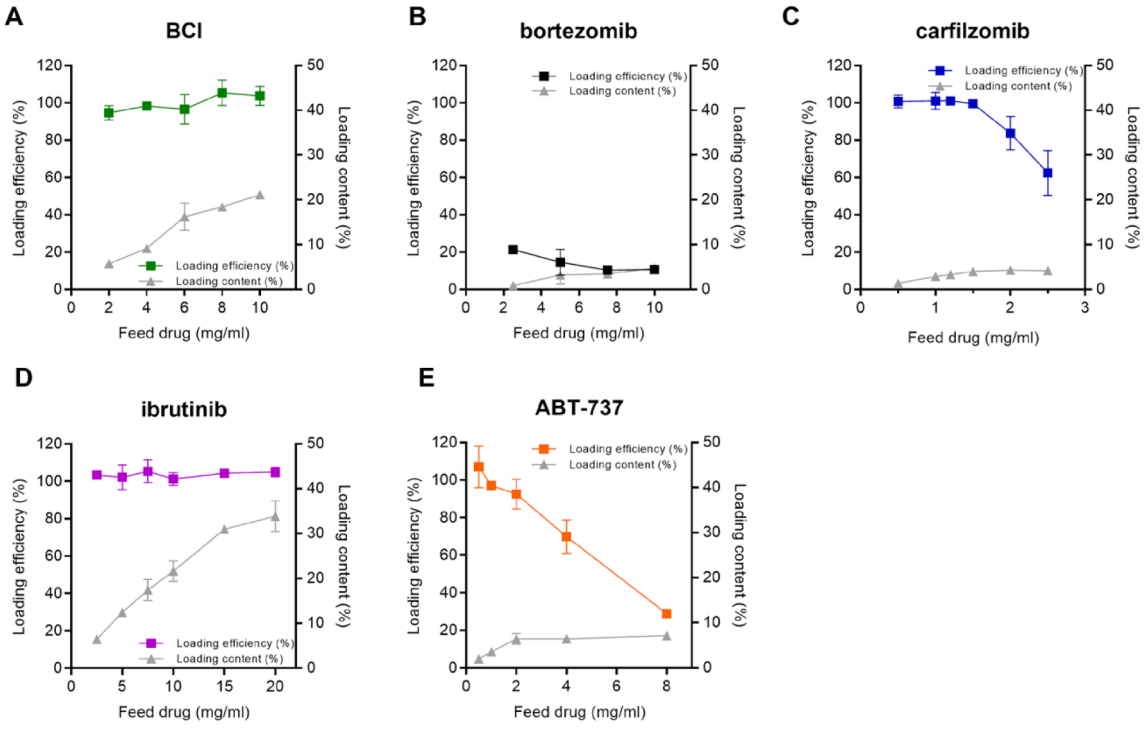

Fig. 4. Loading efficiency and content of polymeric micelles loaded with different hydrophobic anti-cancer drugs. The amount of loaded drug in the micelles was quantified by HPLC/UPLC as described in the SI. Data are presented as mean ± SD, n = 3.

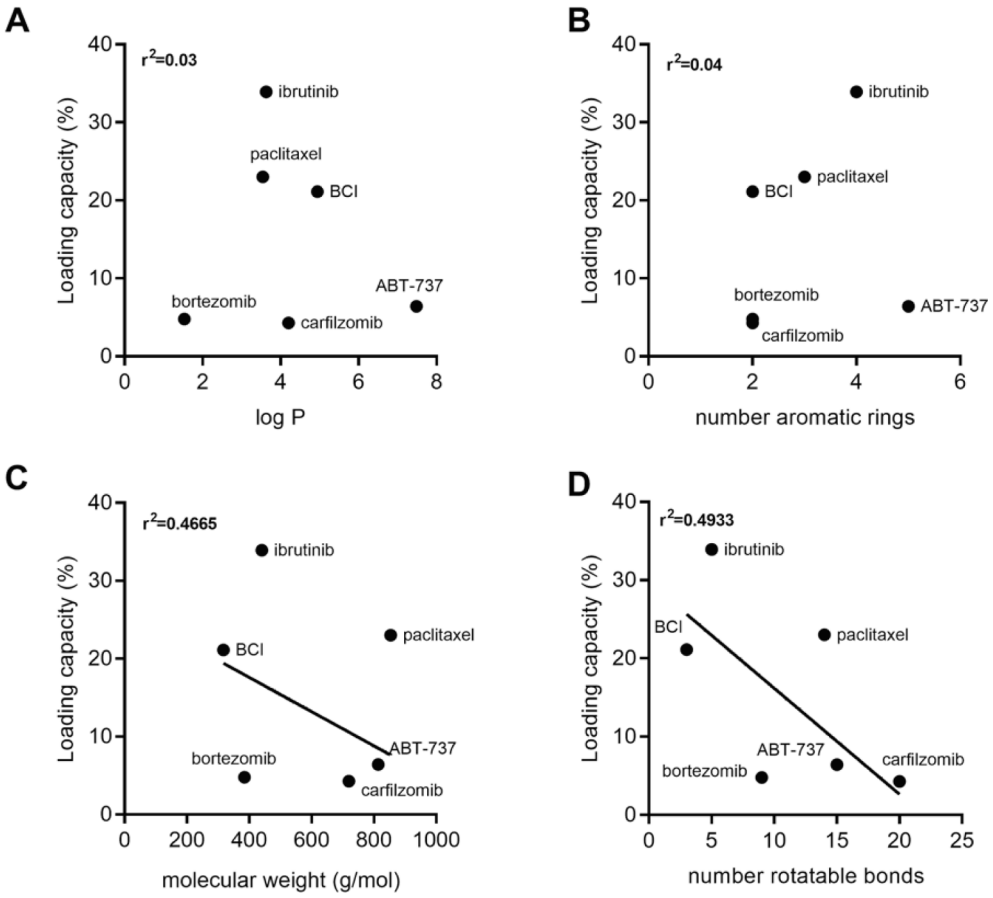

Fig. 5. Drug loading capacity of polymeric micelles as a function of (A) logP, (B) number of aromatic rings, (C) molecular weight and (D) number of rotatable bonds of the drugs – BCI, ibrutinib, bortezomib, carfilzomib, ABT-737 and paclitaxel.

whole blood centrifugation (2000*g* for 5 min at 20 °C) and stored at −80 °C until further use. To extract ABT-737 from plasma, 1 vol of plasma was mixed with 9 volumes of methanol: acetonitrile (1:1, v/v) and vortexed for 1 min for plasma protein precipitation. Next, samples were centrifuged at 12,000*g* for 15 min and the supernatant collected to determine ABT-737 concentration by HPLC as described in SI. For BCI quantification, 1 vol of plasma was mixed with 9 volumes of ACN and vortexed for 1 min for plasma proteins precipitation. Samples were centrifuged at 12,000*g* for 15 min and the supernatant was collected for quantitation of BCI concentration in plasma by HPLC as described in SI. The method to extract ABT-737 and BCI from plasma was validated by spiking known amounts of drug with plasma, followed by precipitation of albumin and determination of the drug concentration in the supernatant. Full recovery of the drugs was obtained.

Fluorescence of Cy7-PM was detected in plasma by a fluorescence scanner Odyssey® (LI-COR Westburg, the Netherlands). Plasma was diluted in PBS prior to fluorescence detection. A calibration curve was prepared with Cy7-labelled polymer (synthesized as previously described (Shi et al., 2015)) dissolved in DMSO and subsequently diluted in PBS at concentrations between 0.01 and 100 μg/mL.

2.4. Statistical analysis

Statistical analysis was performed by GraphPad Prism software version 7.04 (GraphPad Software, Inc., La Jolla, CA, USA). Correlation between the variables was assessed with linear regression, exhibiting the r^2 as a measure of the degree of correlation between the analyzed data.

3. Results and discussion

3.1. Characterization of drug-loaded polymeric micelles

The average diameter of PM loaded with different drugs and prepared at different feeds was determined by DLS. BCI-PM (Fig. 3A) showed a dose-dependent increase in average size from 55 to 75 nm, with a concomitant slight increase in PDI. PTX-PM, as previously reported, also showed an increase in size from 80 to 100 nm upon increasing feed ratios (Shi et al., 2015). In contrast, PM loaded with bortezomib, carfilzomib, ibrutinib and ABT-737 presented very stable sizes around 55 nm and low polydispersity index (PDI < 0.10) for all feed drug ratios tested (Fig. 3B-E). Previously, we have also confirmed this by electron microscopy (Bagheri et al., 2018).

Loading efficiency and loading content are shown in Fig. 4. Besides bortezomib, all drugs were efficiently loaded into the core of PM with an encapsulation efficiency (EE) reaching 80–100% of the amount of drug in the feed. BCI and ibrutinib (Fig. 4A and 4D) showed good loading efficiencies close to 100% for all feed ratios investigated. Although BCI is charged at pH 7.4, this does not negatively influence its loading in PM (Table 1). Apparently, despite its charge, the drug molecule is sufficiently hydrophobic for solubilization in the core of the micelles. In addition, the hydrophobic environment of the core might lower the pK_a of the amine group of the drug. Fig. 4A and 4D show that the loading content increased with increasing drug feed, reaching up to 21 and 34 wt % for BCI and ibrutinib, respectively. We have previously shown that PTX has good loading efficiency and high loading content up to 23 wt% (Shi et al., 2015). Bortezomib (Fig. 4B) was not efficiently encapsulated in PM and displayed low loading efficiency (<20%) and consequently low loading capacity – 5 wt%. Carfilzomib and ABT-737 were efficiently

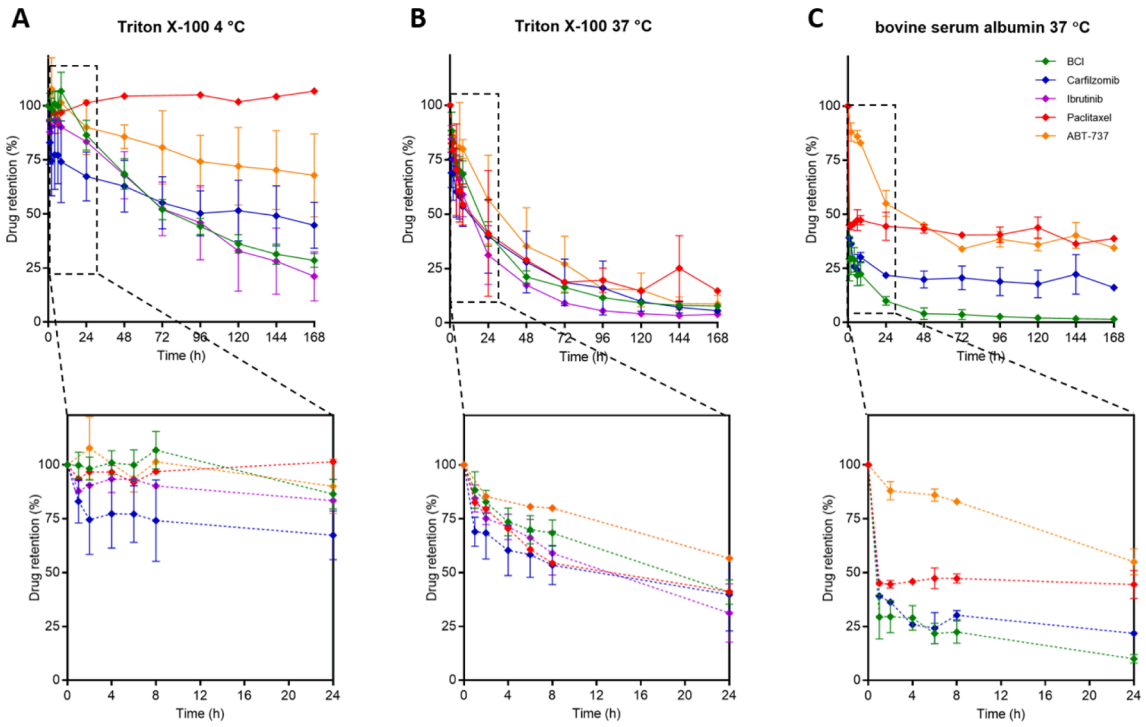

Fig. 6. Retention of hydrophobic drugs in polymeric micelles over 168 h in different media. Drug loaded polymeric micelles were prepared at 6, 1, 5, 1 and 6 mg/mL of BCI, carfilzomib, ibrutinib, ABT-737 and PTX, respectively, and 30 mg/mL of polymer – at loading efficiencies close to 100%. Drug-loaded PM were transferred into a dialysis cassette and incubated either with Triton X-100 (2% v/v in PBS; 30 mL) at 4 °C (A) and at 37 °C (B) or with bovine serum albumin (40 g/L in PBS; 30 mL) at 37 °C (C). At predetermined timepoints ranging from 1 to 168 h, samples of 10 μL of the dispersion inside the dialysis tube were collected and analyzed by HPLC or UPLC to determine the percentage of drug that retained in the micelles compared to the total amount added at the start of the experiment. Data are shown as mean ± SD, n = 3 for the assay using Triton X-100 and n = 2 for the assay using albumin as solubilizer/acceptor.

loaded in the core of PM up to a feed drug concentration of 1.5–2 mg/mL (Fig. 4C and E). Although carfilzomib and ABT-737 were not entrapped in high payloads into PM, at low feed drug concentrations (up to 2 mg/mL) these were well encapsulated in PM (>80%), indicating that these drugs are good candidates for further testing.

Poor drug loading and retention in PM are regarded as one of the major drawbacks hampering their clinical application (Zhang et al., 2017; Houdaihed et al., 2017a). To investigate this aspect, PM at a fixed polymer concentration (30 mg/mL) were loaded with increasing amounts of the drugs listed in Table 1. Loading efficiency and content were determined and showed in Fig. 4. When the loading content reaches a plateau – indicating the drug saturation of the micellar system - this is considered the loading capacity (LC), as the maximum amount (in mass) of drug that the micellar system can accommodate. LogP is commonly used to define the hydrophobicity of a drug. Fig. 5A shows that there is no correlation between the loading capacity and logP of the tested drugs. Yet is logical to assume that drugs with low logP do not partition efficiently in the core of PM. Bortezomib, with logP of 1.5, showed loading efficiency below 20 wt% for all feed drug tested (Fig. 4 B). Even though bortezomib has two aromatic rings, the molecule clearly lacks hydrophobicity to be solubilized in the hydrophobic core of PM. Luxenhofer and colleagues found similar results with dexamethasone (logP of 1.68) loaded in triblock copolymers-based micelles containing benzyl or phenyl moieties in the core (loading efficiency < 30% and loading content < 5.6%) (Lübtow et al., 2019).

The number of aromatic rings are considered an important factor for loading of drugs in mPEG-b-p(HPMA-Bz)-based PM because these moieties could be involved in π-π stacking (Cao et al., 2014; Chen et al., 2018; Zhuang et al., 2019). This was previously hypothesized as the driving force for drug loading in mPEG-b-p(HMPA-Bz)-based PM (Shi et al., 2015). There is no apparent correlation between the number of aromatic rings and loading capacity, as depicted in Fig. 5 B. BCI, bortezomib and carfilzomib, with two aromatic rings, display different loading capacities. Thus, the aromatic content of drugs is probably not the major property of drugs to influence the loading in PM. Analysis of the physicochemical properties of BCI, bortezomib and carfilzomib (Table 1), we can hypothesize that low loading capacity of bortezomib is likely due to low logP value, as discussed above. BCI and carfilzomib largely differ in molecular weight and number of rotatable bounds (molecular weight of 317 and 720 g/mol and number of rotatable bounds 3 and 20, respectively). Consequently, these parameters can also have an effect in the loading of these drugs in PM. Linear regression analysis showed a modest negative correlation between loading capacity and molecular weight ($r^2 = 0.47$, Fig. 5 C). Drugs with large molecular weights (ABT-737 and carfilzomib) showed lowest loading capacity, whereas BCI and ibrutinib, that present roughly half of that molecular weight, showed highest loading capacity. Plotting loading capacity expressed in moles of drug per gram of polymer, the correlation between loading capacity and molecular weight of drugs becomes more evident ($r^2 = 0.60$, Fig. S1). PM can solubilize more drug molecules of low molecular weight drugs per gram of polymer as compared to high molecular weight drugs.

The number of rotatable bonds measures the molecular flexibility of hydrophobic drugs (Clark et al., 1993). This is defined as any single bond, that is not present in a ring structure, bound to a nonterminal non-hydrogen atom (Veber et al., 2002). Linear regression analysis showed a modest negative correlation between loading capacity and number rotatable bonds ($r^2 = 0.49$, Fig. 5 D). Drugs with a relatively high number of rotatable bounds, i.e., ABT-737 and carfilzomib, presented the lowest loading capacity. With an increase in number of rotatable bonds, the molecular flexibility also increases and consequently the association strength between molecules is reduced (von der Lieth et al., 1996). Since high molecular weight drugs are more likely to have higher numbers of rotatable bonds (Fig. S2) these parameters are interrelated

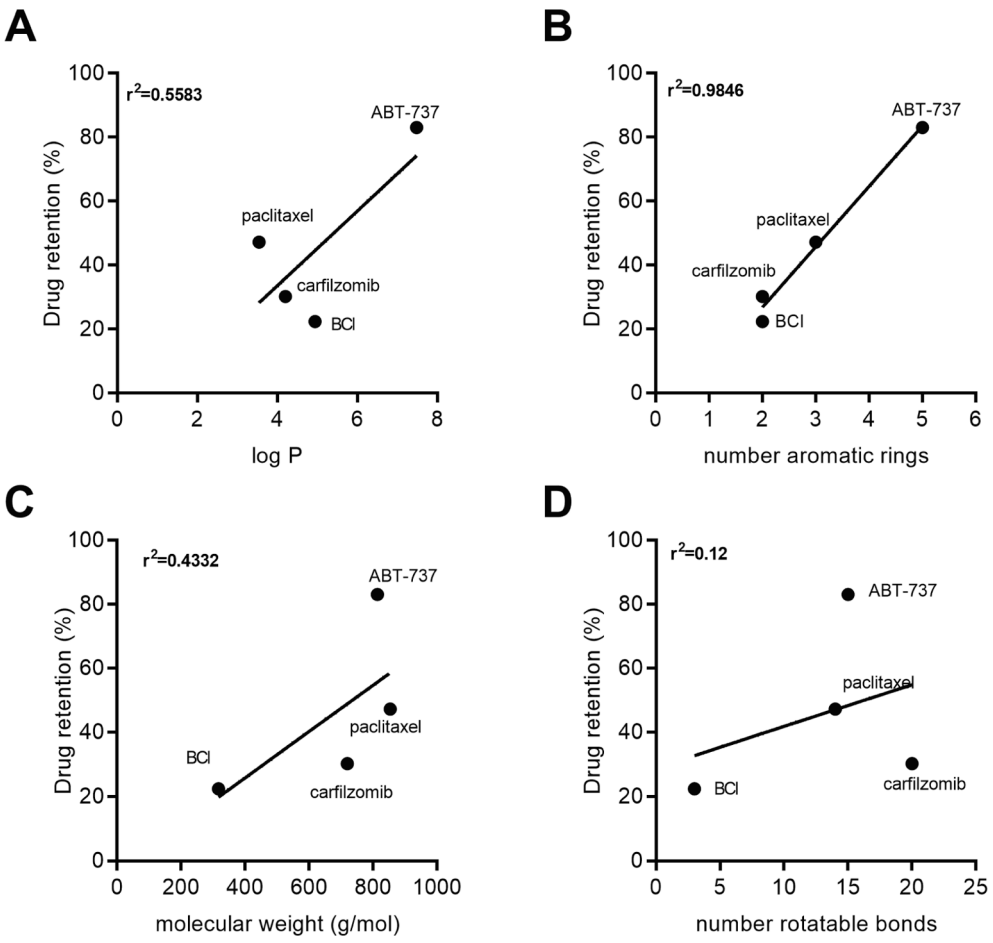

Fig. 7. Drug retention in PM after 8 h incubation of drug loaded polymeric micelles with bovine serum albumin (40 g/L in PBS; 30 mL) at 37 °C as a function of (A) logP, (B) number of aromatic rings, (C) molecular weight and (D) number of rotatable bonds of the studied drugs – BCI, carfilzomib, ABT-737 and paclitaxel. The molar ratio between albumin and drugs was between 2 and 30 meaning that an excess of albumin was present, when compared to the number of moles of the drugs here tested.

and should be cautiously interpreted as separate parameters.

3.2. Drug retention in polymeric micelles

Prolonged circulation time in blood and targeted tissue accumulation are two features aimed for developing an efficient drug carrier system. To benefit from these characteristics, not only good accommodation of hydrophobic drugs in the core is essential, but sufficient drug retention upon micellar distribution in physiological milieu is crucial (Wilhelm et al., 2016). Here we investigated the drug release from PM in buffer containing Triton X-100 (2%, v/v) (Naksuriya et al., 2015). Triton X-100 is a surfactant that forms small (±10 nm) micelles in water (Fig. S3A) which can solubilize ('capture') released drugs in the aqueous acceptor phase and thus act as a sink. Importantly, in agreement with previous findings, Triton X-100 micelles did not mix/fuse with drug-loaded PM (Fig. S3B and S3C) (Naksuriya et al., 2015). Dialysis cassettes of 100 kDa MWCO were used to allow Triton X-100 micelles to freely move between inside and outside of the dialysis cassette. We showed that when the used dialysis membrane is impermeable for Triton X-100 micelles, the drug retention in PM appears substantially higher (Fig. S4A) (Chen et al., 2008).

Fig. 6 shows the retention of drugs in PM over 168 h. BCI, carfilzomib, ibrutinib, ABT-737 and PTX were loaded in PM at concentrations below the maximum loading content to prevent overloading of the micellar system, which were 6, 1, 5, 1 and 6 mg/mL, polymer concentration 30 mg/mL, respectively. Bortezomib was excluded from these experiments as it showed poor drug loading in PM and thus does not represent a promising candidate to formulate in PM. When drug-loaded PM were incubated in buffer containing Triton X-100 micelles at 4 °C they showed the highest retention of the payload, with more than 60% of the initially added drug retained in PM 24 h after incubation (Fig. 6A). In the same Triton X-100-containing buffer and at body temperature – 37 °C -, drug release was considerably faster (Fig. 6B). Under these conditions and after 24 h of incubation, more than 50% of the loaded BCI, carfilzomib, ibrutinib and paclitaxel was released from PM. The lower retention observed at 37 °C than at 4 °C can be attributed to the higher solubility of drug molecules at elevated temperatures. The increase in solubility facilitates the transfer of drug molecules from the hydrophobic core of PM to the aqueous environment (Kastantin et al., 2012). Faster release of drugs from PM at higher temperatures was also previously reported (Zhao et al., 2016). Interestingly, no striking differences were observed in the release profiles between different drugs tested (Fig. 6B).

In addition, drug retention was determined in the presence of albumin, at the concentration present in human plasma (40 g/L in PBS pH 7.4), since this is the most abundant plasma protein and has hydrophobic pockets able to accommodate hydrophobic drugs (Kim et al., 2010; Sułkowska, 2002). For BCI and carfilzomib, rapid drug release/extraction (greater than60%) from PM was observed after 1 h of incubation at 37 °C in the presence of albumin (Fig. 6C). After 24 h incubation of PM with albumin, 10–20% of the loaded drug was retained in the core of the micelles loaded with BCI and carfilzomib, respectively. 50% of PTX content was released in the first hour of incubation with albumin, while thereafter no further release occurred. Shi *et al.* prepared PTX-PM at 3.2 mg/mL of PTX (27 mg/mL of polymer) and showed high stability of the micellar system in circulation (Shi et al., 2015) while in present study the release in albumin of a similar micellar formulation was evaluated at 6 mg/mL of PTX (30 mg/mL of polymer). Thus, the initial fast extraction of 50% of the loaded PTX might be due to overloading of PM. Recently, Sheybanifard M. *et al* showed no differences in

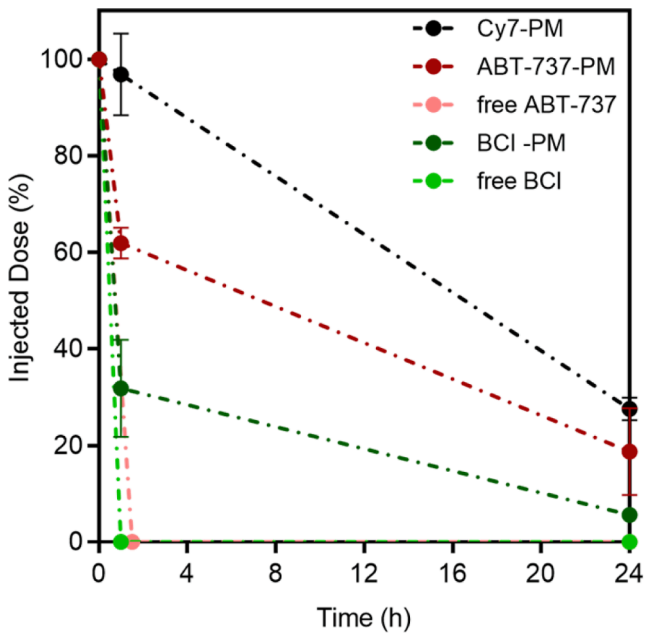

Fig. 8. Circulation time in blood of ABT-737, BCI and Cy7-labelled PM. Immunocompetent mice were i.v. injected with free ABT-737 or ABT-737-PM, and free BCI or BCI-PM via the tail vein. At 1 min, 1 and 24 h blood was withdrawn to determine the percentage of injected dose (%ID) present in the circulation. Blood collected shortly after injection (1 min) was considered as 100% ID. Fluorescence intensity of Cy7-PM in plasma was measured in Odyssey® imager. Drug concentrations in plasma were determined by HPLC. Data are presented as mean ± SD, n = 3 for Cy7-PM and BCI, n = 2 for ABT-737.

the release profile of PTX-PM-based on mPEG-b-p(HPMA-Bz) (in PBS with 4.5% BSA as releasing medium) loaded with 5,10 or 15% (w/w) of PTX (Sheybanifard et al., 2020). In the present study we loaded PM with 20% (w/w) PTX which is still below the maximum loading capacity of PTX in this micellar formulation. Hence, further studies are needed to determine whether this initial burst release is due to overloading. Finally, ABT-737-PM displayed sustained release of the drug with a more gradual release observed and with 55% of the initial loaded drug retained in PM after 24 h incubation with albumin, that remained stable throughout the seven days of analysis (Fig. 6C). Although an excess of moles of albumin of at least 2-fold compared to the moles of drug, 48 h after incubation, the release from the dialysis membrane plateaus.

The percentage of drug retained in PM after 8 h incubation with albumin is plotted as a function of the physicochemical properties of the drugs tested (Fig. 7). This time point was chosen as it showed the highest discriminatory value. LogP values showed a positively correlation to the drug retention in PM (Fig. 7A), indicating that the (lack of) water solubility is important for drug retention in PM. Strikingly, the number of aromatic moieties almost perfectly correlates ($r^2 = 0.98$) with the percentage of drug that retained in the core of PM (Fig. 7B), suggesting that π-π interactions between polymer and loaded drug molecules play an important role in this process. The molecular weight also positively correlates to drug retention in PM, although to a lesser extent ($r^2 = 0.43$, Fig. 7C). Again, aromatic content, molecular weight and logP could be considered as confounding factors, but the near perfect correlation with the number of aromatic moieties indicates this is the dominant parameter. Finally, no correlation is observed between drug retention and number of rotatable bonds (Fig. 7D).

3.3. Circulation time of drug-loaded polymeric micelles

In vitro release assays are employed to predict stability and drug release *in vivo* of drug loaded PM. Undeniably, it is challenging to mimic *in vivo* conditions such as the blood flow and blood composition by means of an *in vitro* release assay. Moreover, technical difficulties remain like the separation of (hydrophobic) drugs loaded in PM, and protein-bound (hydrophobic) drugs released from PM. Here, we selected two drugs that showed particularly different release profiles *in vitro*, namely ABT-737 and BCI (Fig. 6C) and evaluated their circulation time as micellar formulation *in vivo*. We examined the circulation time of Cy7-labeled PM loaded with either ABT-737 or BCI (at 1 and 6 mg/mL, respectively; 30 mg/mL of polymer) in healthy immunocompetent mice and compared these to the drug retention in PM found in the *in vitro* release assays (ABT-737 and BCI showed 55 and 10% of drug retention in albumin containing buffer after 24 h incubation, respectively). Fig. 8 shows that Cy7-labeled PM showed prolonged blood residence with 28% of the injected dose (ID) still in circulation 24 h after i.v. administration, which is similar to the circulation kinetics previously reported for the same micellar system (Shi et al., 2015). When loaded in PM, ABT-737 was better retained than BCI in peripheral blood. ABT-737 displayed prolonged circulation time in plasma with 62% and 19% ID in circulation at 1 and 24 h post-injection, respectively (Fig. 8). BCI-PM showed faster drug loss/extraction *in vivo*, since at 1 and 24 h post administration 32 and 6% ID, respectively, was detected in the circulation. ABT-737 and BCI when administered as free drugs (dissolved in 100% DMSO and administered in PBS with < 1% (v/v) of DMSO) were rapidly

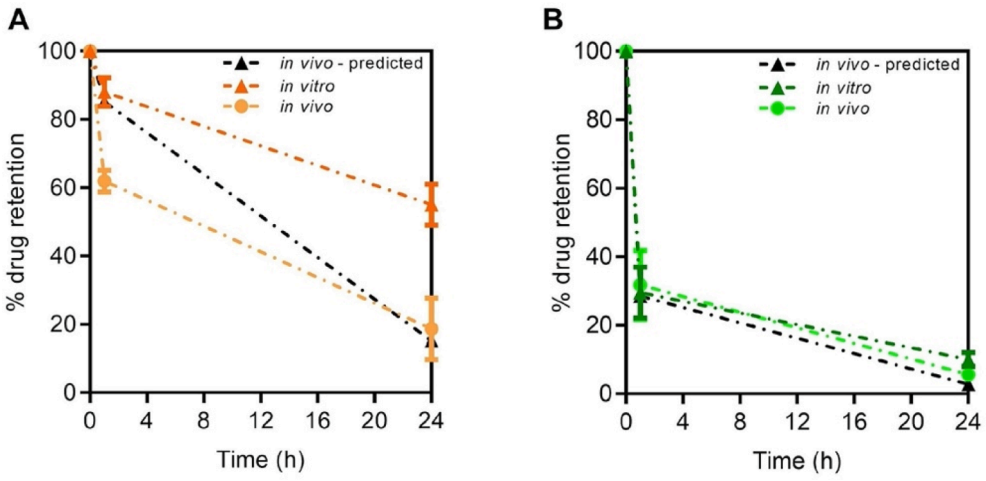

Fig. 9. Comparison of drug retention in polymeric micelles determined *in vitro* (in release medium containing BSA), *in vivo* (circulation time in plasma) and the predicted *in vivo* retention calculated based on the detected %ID of Cy7-PM at each time point (1 h and 24 h). The detected %ID of PM at 1 h and 24 h was used to correct for the maximum drug detectable amount in blood; (A) ABT-737 polymeric micelles and (B) BCI polymeric micelles.

eliminated and after 1 h no drug was detected in the analyzed plasmas. This is due to strong binding of ABT-737 to albumin present in blood (Vogler et al., 2010). BCI is a drug recently developed (Molina et al., 2009) and no studies can be found on its elimination kinetics *in vivo*. However, the fast elimination we observe is most likely due to strong binding to hydrophilic surfaces, as lipoproteins.

As expected, drug retention *in vivo* was lower when compared to drug retention found *in vitro* in the presence of albumin containing medium. One of the differences between both experimental set-ups is that plasma composition comprises other hydrophobic proteins, such as apolipoproteins, rather than only albumin (Zhao et al., 2016). Also, *in vivo* part of PM "leaves" systemic circulation and accumulate in tissues contributing to an apparent loss of retention. Taking this into account, we recalculated drug retention *in vivo* and used the detected % ID of Cy7-labeled PM at 1 h and 24 h (which was 97 and 28% ID, respectively) to correct for the maximum drug amount detectable in blood as 100% of micelles in circulation at that timepoint (Fig. 9). At 1 h, 97% ID of Cy7-PM are in circulation. At the same timepoint, based on our *in vitro* release assay, 88% and 29% of initial ABT-737 and BCI, respectively, are retained in PM. Based on *in vitro* retention, we estimate that the *in vivo* retention of ABT-737 and BCI is of 85 and 28.5% (Fig. 9 and Table S1). Our prediction is close to our *in vivo* findings, since we detected 62 and 32% ID of ABT-737 and BCI. At 24 h, based on the remainder Cy7-PM in circulation (=28% ID), we predicted that 2.8 and 15% ID of BCI and ABT-737, respectively, was retained in PM. These figures are close to the percentage of BCI and ABT-737 retained *in vivo*, i.e., 5.6 and 19% (Fig. 9, Table S1). The same calculation was performed for PTX-PM, given Cy7-PM and PTX circulation in blood 24 h after i.v. administration, as reported in (Shi et al., 2015), which amounted to 20 and 10% ID, respectively. Considering PTX-PM in circulation at 24 h, 50% of feed PTX was retained in the PM, which was the same figure we found for *in vitro* retention with albumin (Fig. 6C). Thus, with the *in vitro* release assay based on albumin as acceptor protein here developed, we can find a good estimation of drug retention upon i.v. administration of PM formulations based on mPEG-b-p(HPMA-Bz).

4. Conclusions

In this study, we evaluated the *in vitro* loading and retention as well as the *in vivo* pharmacokinetics of a panel of hydrophobic drugs containing aromatic moieties loaded in mPEG-b-p(HPMA-Bz)-based micelles. By using the collected information, the correlation between the different drugs regarding several physicochemical properties could be determined. Interestingly, we found that a few parameters potentially affect loading and retention of hydrophobic drugs in PM. High logP is important for good loading efficiency. As expected, high logP is also important to retain the drug in the core of PM. Strikingly, *in vitro* drug retention in PM shows high correlation with the aromatic content of the tested drugs. Finally, we analyzed the *in vivo* circulation kinetics of two selected drugs and compared these results with *in vitro* release profiles. The two selected drugs exhibited similar drug retention *in vivo* in mice as we found with *in vitro* assay based on albumin (after correcting the Cy7-PM %ID in circulation at each time point). Our findings support the possibility of replacing, when possible, the use of animals for PK studies with validated *in vitro* assays. This approach can be applied as a first *in vitro* screen to test potential drugs assisting in the detection of poorly performing drugs prematurely. With this, we narrow the number of drugs further tested through *in vivo* pharmacokinetic studies and, consequently, contribute to the reduction (one of the 3R's) of the number of animals used for PK-related studies.

CRediT authorship contribution statement

Aida Varela-Moreira: Formal analysis, Investigation, Writing – original draft. **Heleen van Leur:** Investigation. **Danielle Krijgsman:** Investigation. **Veronika Ecker:** Investigation. **Martina Braun:** Investigation. **Maike Buchner:** Investigation, Writing – review & editing. **Marcel H.A.M. Fens:** Conceptualization, Supervision, Writing – review & editing. **Wim E. Hennink:** Conceptualization, Supervision, Writing – review & editing. **Raymond M. Schiffelers:** Conceptualization, Supervision, Writing – review & editing.

Declaration of Competing Interest

The authors declare that they have no known competing financial interests or personal relationships that could have appeared to influence the work reported in this paper.

Acknowledgments

This work was funded by Netherlands Organization for Scientific Research (NWO), High Tech Systems & Materials grant number 13312.

Appendix A. Supplementary material

Supplementary data to this article can be found online at https://doi.org/10.1016/j.ijpharm.2022.121638.

References

Bagheri, M., Bresseleers, J., Varela-Moreira, A., Sandre, O., Meeuwissen, S.A., Schiffelers, R.M., Metselaar, J.M., van Nostrum, C.F., van Hest, J.C.M., Hennink, W. E., 2018. Effect of formulation and processing parameters on the size of mpeg-b-p (hpma-bz) polymeric micelles. Langmuir 34 (50), 15495–15506. https://doi.org/10.1021/acs.langmuir.8b0357610.1021/acs.langmuir.8b03576.s001.

Cabral, H., Miyata, K., Osada, K., Kataoka, K., 2018. Block copolymer micelles in nanomedicine applications. Chem. Rev. 118 (14), 6844–6892. https://doi.org/10.1021/acs.chemrev.8b00199.

Cai, R., Chen, C., 2019. The crown and the scepter: Roles of the protein corona in nanomedicine. Adv. Mater. 31 (45), 1805740. https://doi.org/10.1002/adma.201805740.

Cao, M., Fu, A., Wang, Z., Liu, J., Kong, N.a., Zong, X., Liu, H., Gooding, J.J., 2014. Electrochemical and theoretical study of π–π stacking interactions between graphitic surfaces and pyrene derivatives. J. Phys. Chem. C 118 (5), 2650–2659. https://doi.org/10.1021/jp411979x.

Chen, H., Kim, S., Li, L., et al., 2008. Release of hydrophobic molecules from polymer micelles into cell membranes revealed by forster resonance energy transfer imaging. Proc. Natl. Acad. Sci. U S A 105, 6596–6601. https://doi.org/10.1073/pnas.0707046105.

Chen, T., Li, M., Liu, J., 2018. Π–π stacking interaction: A nondestructive and facile means in material engineering for bioapplications. Cryst. Growth Des. 18 (5), 2765–2783. https://doi.org/10.1021/acs.cgd.7b01503.

Clark, D.E., Willett, P., Kenny, P.W., 1993. Pharmacophoric pattern matching in files of three-dimensional chemical structures: Implementation of flexible searching. J. Mol. Graph. 11 (3), 146–156. https://doi.org/10.1016/0263-7855(93)80066-Z.

Deng, C., Jiang, Y., Cheng, R.u., Meng, F., Zhong, Z., 2012. Biodegradable polymeric micelles for targeted and controlled anticancer drug delivery: Promises, progress and prospects. Nano Today 7 (5), 467–480. https://doi.org/10.1016/j.nantod.2012.08.005.

Houdaihed, L., Evans, J.C., Allen, C., 2017. Overcoming the road blocks: Advancement of block copolymer micelles for cancer therapy in the clinic. Mol. Pharm. 14 (8), 2503–2517. https://doi.org/10.1021/acs.molpharmaceut.7b00188.

Jones, M.-C., Leroux, J.-C., 1999. Polymeric micelles - a new generation of colloidal drug carriers. Eur. J. Pharm. Biopharm. 48 (2), 101–111.

Kalepu, S., Nekkanti, V., 2015. Insoluble drug delivery strategies: Review of recent advances and business prospects. Acta Pharmaceut. Sinica B 5 (5), 442–453.

Kastantin, M., Walder, R., Schwartz, D.K., 2012. Identifying mechanisms of interfacial dynamics using single-molecule tracking. Langmuir 28 (34), 12443–12456. https://doi.org/10.1021/la3017134.

Kim, S., Shi, Y., Kim, J.Y., Park, K., Cheng, J.-X., 2010. Overcoming the barriers in micellar drug delivery: Loading efficiency, in vivo stability, and micelle-cell interaction. Expert Opin Drug Deliv 7 (1), 49–62. https://doi.org/10.1517/17425240903380446.

Lammers, T., 2019. Macro-nanomedicine: Targeting the big picture. J. Control. Release 294, 372–375. https://doi.org/10.1016/j.jconrel.2018.11.031.

Lee, H., Hoang, B., Fonge, H., Reilly, R.M., Allen, C., 2010. In vivo distribution of polymeric nanoparticles at the whole-body, tumor, and cellular levels. Pharm. Res. 27 (11), 2343–2355. https://doi.org/10.1007/s11095-010-0068-z.

Lipinski, C.A., 2000. Drug-like properties and the causes of poor solubility and poor permeability. J. Pharmacol. Toxicol. Methods 44 (1), 235–249.

Lübtow, M.M., Haider, M.S., Kirsch, M., Klisch, S., Luxenhofer, R., 2019. Like dissolves like? A comprehensive evaluation of partial solubility parameters to predict polymer-drug compatibility in ultrahigh drug-loaded polymer micelles. Biomacromolecules 20 (8), 3041–3056. https://doi.org/10.1021/acs.biomac.9b0061810.1021/acs.biomac.9b00618.s001.

Maeda, H., Wu, J., Sawa, T., Matsumura, Y., Hori, K., 2000. Tumor vascular permeability and the epr effect in macromolecular therapeutics: A review. J. Control. Release 65 (1-2), 271–284. https://doi.org/10.1016/S0168-3659(99)00248-5.

Molina, G., Vogt, A., Bakan, A., Dai, W., de Oliveira, P.Q., Znosko, W., Smithgall, T.E., Bahar, I., Lazo, J.S., Day, B.W., Tsang, M., 2009. Zebrafish chemical screening reveals an inhibitor of dusp6 that expands cardiac cell lineages. Nat. Chem. Biol. 5 (9), 680–687. https://doi.org/10.1038/nchembio.190.

Naksuriya, O., Shi, Y., van Nostrum, C.F., Anuchapreeda, S., Hennink, W.E., Okonogi, S., 2015. Hpma-based polymeric micelles for curcumin solubilization and inhibition of cancer cell growth. Eur. J. Pharm. Biopharm. 94, 501–512. https://doi.org/10.1016/j.ejpb.2015.06.010.

Sakai-Kato, K., Nishiyama, N., Kozaki, M., Nakanishi, T., Matsuda, Y., Hirano, M., Hanada, H., Hisada, S., Onodera, H., Harashima, H., Matsumura, Y., Kataoka, K., Goda, Y., Okuda, H., Kawanishi, T., 2015. General considerations regarding the in vitro and in vivo properties of block copolymer micelle products and their evaluation. J. Control. Release 210, 76–83. https://doi.org/10.1016/j.jconrel.2015.05.259.

Sharifi, S., Caracciolo, G., Mahmoudi, M., 2020. Biomolecular corona affects controlled release of drug payloads from nanocarriers. Trends Pharmacol. Sci. 41 (9), 641–652. https://doi.org/10.1016/j.tips.2020.06.011.

Sheybanifard, M., Beztsinna, N., Bagheri, M., Buhl, E.M., Bresseleers, J., Varela-Moreira, A., Shi, Y., van Nostrum, C.F., van der Pluijm, G., Storm, G., Hennink, W.E., Lammers, T., Metselaar, J.M., 2020. Systematic evaluation of design features enables efficient selection of π electron-stabilized polymeric micelles. Int. J. Pharm. 584, 119409. https://doi.org/10.1016/j.ijpharm.2020.119409.

Shi, Y., van der Meel, R., Theek, B., et al., 2015. Complete regression of xenograft tumors upon targeted delivery of paclitaxel via pi-pi stacking stabilized polymeric micelles. ACS Nano 9, 3740–3752. https://doi.org/10.1021/acsnano.5b00929.

Shi, Y., Lammers, T., Storm, G., et al., 2017. Physico-chemical strategies to enhance stability and drug retention of polymeric micelles for tumor-targeted drug delivery. Macromol. Biosci. 17, 1600160. https://doi.org/10.1002/mabi.201600160.

Sudlow, G., Birkett, D.J., Wade, D.N., 1975. The characterization of two specific drug binding sites on human serum albumin. Mol. Pharmacol. 11, 824–832.

Sudlow, G., Birkett, D.J., Wade, D.N., 1976. Further characterization of specific drug binding sites on human serum albumin. Mol. Pharmacol. 12, 1052–1061.

Sułkowska, A., 2002. Interaction of drugs with bovine and human serum albumin. J. Mol. Struct. 614 (1-3), 227–232. https://doi.org/10.1016/S0022-2860(02)00256-9.

Takagi, T., Ramachandran, C., Bermejo, M., Yamashita, S., Yu, L.X., Amidon, G.L., 2006. A provisional biopharmaceutical classification of the top 200 oral drug products in the united states, great britain, spain, and japan. Mol. Pharm. 3 (6), 631–643. https://doi.org/10.1021/mp060018210.1021/mp0600182.s001.

Talelli, M., Iman, M., Varkouhi, A.K., Rijcken, C.J.F., Schiffelers, R.M., Etrych, T., Ulbrich, K., van Nostrum, C.F., Lammers, T., Storm, G., Hennink, W.E., 2010. Core-crosslinked polymeric micelles with controlled release of covalently entrapped doxorubicin. Biomaterials 31 (30), 7797–7804. https://doi.org/10.1016/j.biomaterials.2010.07.005.

Talelli, M., Rijcken, C.J.F., Hennink, W.E., Lammers, T., 2012. Polymeric micelles for cancer therapy: 3 c's to enhance efficacy. Curr. Opin. Solid State Mater. Sci. 16 (6), 302–309. https://doi.org/10.1016/j.cossms.2012.10.003.

van Nostrum, C.F., 2011. Covalently cross-linked amphiphilic block copolymer micelles. Soft Matter 7, 3246–3259. https://doi.org/10.1039/C0SM00999G.

Varela-Moreira, A., Shi, Y., Fens, M.H.A.M., Lammers, T., Hennink, W.E., Schiffelers, R.M., 2017. Clinical application of polymeric micelles for the treatment of cancer. Mater. Chem. Front. 1 (8), 1485–1501. https://doi.org/10.1039/C6QM00289G.

Veber, D.F., Johnson, S.R., Cheng, H.-Y., Smith, B.R., Ward, K.W., Kopple, K.D., 2002. Molecular properties that influence the oral bioavailability of drug candidates. J. Med. Chem. 45 (12), 2615–2623. https://doi.org/10.1021/jm020017n.

Vogler, M., Furdas, S.D., Jung, M., Kuwana, T., Dyer, M.J.S., Cohen, G.M., 2010. Diminished sensitivity of chronic lymphocytic leukemia cells to abt-737 and abt-263 due to albumin binding in blood. Clin. Cancer Res. 16 (16), 4217–4225.

von der Lieth, C.-W., Stumpf-Nothof, K., Prior, U., 1996. A bond flexibility index derived from the constitution of molecules. J. Chem. Inf. Comput. Sci. 36 (4), 711–716. https://doi.org/10.1021/ci9501204.

Wilhelm, S., Tavares, A.J., Dai, Q., Ohta, S., Audet, J., Dvorak, H.F., Chan, W.C.W., 2016. Analysis of nanoparticle delivery to tumours. Nat. Rev. Mater. 1 (5) https://doi.org/10.1038/natrevmats.2016.14.

Yokoyama, M., Fukushima, S., Uehara, R., et al., 1998. Characterization of physical entrapment and chemical conjugation of adriamycin in polymeric micelles and their design for in vivo delivery to a solid tumor. J. Control. Release 50, 79–92. https://doi.org/10.1016/s0168-3659(97)00115-6.

Yuan, X., Jiang, M., Zhao, H., Wang, M., Zhao, Y., Wu, C., 2001. Noncovalently connected polymeric micelles in aqueous medium. Langmuir 17 (20), 6122–6126. https://doi.org/10.1021/la010574x.

Zhang, Y.u., Ren, T., Gou, J., Zhang, L., Tao, X., Tian, B., Tian, P., Yu, D., Song, J., Liu, X., Chao, Y., Xiao, W., Tang, X., 2017. Strategies for improving the payload of small molecular drugs in polymeric micelles. J. Control. Release 261, 352–366. https://doi.org/10.1016/j.jconrel.2017.01.047.

Zhao, Y., Fay, F., Hak, S., Manuel Perez-Aguilar, J., Sanchez-Gaytan, B.L., Goode, B., Duivenvoorden, R., de Lange Davies, C., Bjørkøy, A., Weinstein, H., Fayad, Z.A., Pérez-Medina, C., Mulder, W.J.M., 2016. Augmenting drug-carrier compatibility improves tumour nanotherapy efficacy. Nat. Commun. 7 (1) https://doi.org/10.1038/ncomms11221.

Zhuang, W.-R., Wang, Y.i., Cui, P.-F., Xing, L., Lee, J., Kim, D., Jiang, H.-L., Oh, Y.-K., 2019. Applications of π-π stacking interactions in the design of drug-delivery systems. J. Control. Release 294, 311–326. https://doi.org/10.1016/j.jconrel.2018.12.014.